SLAC-PUB-10707
LCLS-TN-04-11
Revised
October 2004

Resistive wall wakefield in the LCLS undulator beam pipe

Karl L.F. Bane and Gennady Stupakov[†]
Stanford Linear Accelerator Center,
Stanford University, Stanford, CA 94309

Abstract

We have shown that, due to the ac resistive wall wakefield, the present LCLS undulator design, with its round copper beam pipe, will result in an unacceptably large energy variation induced within the bunch over the length of the undulator (0.6%). If, instead, we use a flat, aluminum chamber, the energy variation can be reduced to within acceptable limits ($\lesssim 0.2\%$). Finally we have shown that the effect of the anomalous skin effect in the beam pipe wall is small, and can be ignored.

[†]Work supported by the Department of Energy, contract DE-AC02-76SF00515

I. INTRODUCTION

In the Linac Coherent Light Source (LCLS), the relative energy variation (over the bunch) induced within the undulator region must be kept to a few times the Pierce parameter. If it becomes larger, part of the beam will not reach saturation. The largest contributor to energy change in the undulator region is the (longitudinal) resistive wall wakefield of the copper-coated beam pipe. In this region the LCLS bunch is short (the rms length $\sigma_z = 20$ μm), and the shape can be described as uniform, but with "horns" of charge added at the head and tail. FEL simulations that include the effect of the wake show that—for the portion of beam between the horns—the induced energy variation is acceptable and does not suppress lasing. Until now, however, for resistive wall wake calculations in the LCLS, a formula that includes only the dc conductivity of the metal has been used. In this report we perform more accurate calculations of the wake, ones including also the effect of the ac conductivity in the beam pipe wall.

Electrical (and thermal) conductivity in normal metals can be described quite well up to visible frequencies by the so-called Drude-Sommerfeld free electron model of conductivity (see, *e.g.* Ref. [1]). This model treats conduction electrons as an ideal gas that follows Fermi-Dirac statistics, and it includes as parameters both a dc and an ac conductivity. The dc conductivity of a metal is given by $\sigma = ne^2\tau/m$, with n the density of conduction electrons, e the charge of the electron, τ the relaxation time (or collision time, or mean free time), and m the mass of the electron. The ac conductivity, a response to applied oscillating fields, is given by

$$\tilde{\sigma} = \frac{\sigma}{1 - ikc\tau} \ , \tag{1}$$

where $k = \omega/c$, with ω the frequency of the fields and c the speed of light. Note that for short bunches one needs to include both types of conductivity. For copper at room temperature $c\tau = 8.1$ μm; for a typical bunch frequency of $k \sim 1/\sigma_z = (20\ \mu\text{m})^{-1}$ the second term in the denominator of Eq. 1 equals 0.4 and is not very small compared to the first term; for the actual LCLS bunch shape, with its sharp leading edge, the second term becomes even more important.

The short-range resistive wall wake in a round beam pipe, including ac conductivity, was obtained in Ref. [2]. We here apply the results to the bunch in the LCLS undulator region. To study the effect of a change in shape of the beam pipe cross-section we calculate next the ac wake between parallel resistive plates (or on the axis of a flat beam pipe). In Appendix A, we consider another effect that may be important at high frequencies, the (room temperature) anomalous skin effect, and show that it is, however, small. In Appendix B we perform a parameter study of the ac wakes for both round and flat beam pipes.

Table I gives selected bunch and beam pipe parameters for the LCLS that will be used in our calculations. Note that the inner beam pipe surface is nominally copper.

TABLE I: Selected parameters in LCLS undulator.

Beam energy	E	14.	GeV
Bunch charge	eN	1.	nC
Rms bunch length	σ_z	20.	μm
Beam pipe radius	a	2.5	mm
Beam pipe length	L	130.	m

II. AC CONDUCTIVITY

For a round, metallic beam pipe of radius a and dc conductivity σ the longitudinal impedance is given by [3]

$$Z(k) = \left(\frac{1}{ca}\right) \frac{2}{\frac{\lambda}{k} - \frac{ika}{2}} \ , \tag{2}$$

with parameter λ given by

$$\lambda = \sqrt{\frac{2\pi\sigma|k|}{c}}[i + \mathrm{sign}(k)] \ . \tag{3}$$

(In this report we work in Gaussian units.) The quantity $i\lambda$ is the propagation constant into the metal (the field penetrates as $\sim e^{i\lambda x}$, with x the distance into the metal); the skin depth $\delta = 1/\mathrm{Im}(\lambda)$. The wakefield is given by the inverse Fourier transform of the impedance: [2]–[3]:

$$W(s) = \frac{16}{a^2}\left(\frac{e^{-s/s_0}}{3}\cos\frac{\sqrt{3}s}{s_0} - \frac{\sqrt{2}}{\pi}\int_0^\infty \frac{dx\, x^2 e^{-x^2 s/s_0}}{x^6+8}\right) \ , \tag{4}$$

where s is the distance the test particle is *behind* the exciting charge; with characteristic distance

$$s_0 = \left(\frac{ca^2}{2\pi\sigma}\right)^{\frac{1}{3}} \ . \tag{5}$$

(Positive values indicate voltage loss per unit charge per meter of beam pipe.) Note that $W(s) = 0$ for $s < 0$. For copper $\sigma = 5.8 \times 10^{17}$/s and, with $a = 2.5$ mm, $s_0 = 8.1$ μm. The wake is plotted in Fig. 1. There are two terms in Eq. 4, a resonator term and a non-resonant term. For $s \gg s_0$ the second term dominates and becomes the familiar long range result:

$$W(s) = -\frac{1}{2\pi a}\sqrt{\frac{c}{\sigma}}\frac{1}{s^{3/2}} \ . \tag{6}$$

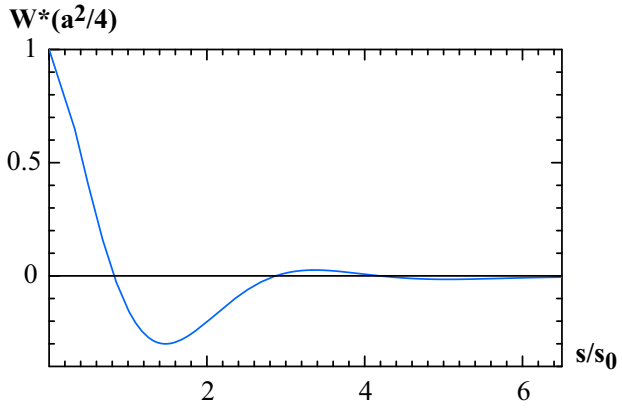

FIG. 1: Resistive wall wake assuming a dc conductivity.

The resistive wall wake including ac conductivity was obtained in Ref. [2]. The calculation is the same as for the dc case, except that σ in the definition of λ (Eq. 3) in the impedance is replaced by the ac conductivity $\tilde{\sigma}$ given in Eq. 1. As an aid to the calculations the result can be written in terms of dimensionless frequency $\kappa = ks_0$ and relaxation time $\Gamma = c\tau/s_0$ [2]:

$$\lambda = \frac{a}{s_0^2}|\kappa|^{1/2}(1+\kappa^2\Gamma^2)^{-1/4}\left[i\sqrt{1+t_\lambda} + \mathrm{sign}(\kappa)\sqrt{1-t_\lambda}\right] \ , \tag{7}$$

with

$$t_\lambda = \frac{|\kappa|\Gamma}{\sqrt{1+\kappa^2\Gamma^2}} \ . \tag{8}$$

Fig. 2 shows the ac impedance for the LCLS beam pipe ($s_0 = 8.1$ μm, $\Gamma = 1.0$), and for comparison also the dc impedance. We note that the resonant peaks of Re(Z) are much narrower in the ac than the dc case.

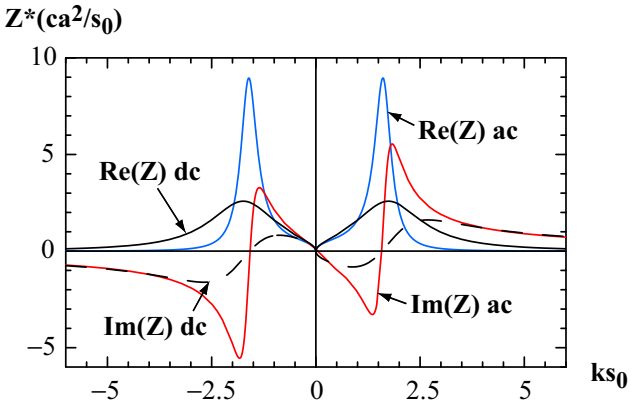

FIG. 2: Real (blue) and imaginary (red) parts of impedance, including ac conductivity, for the LCLS undulator beam pipe. Here $\Gamma = 1.0$. The impedance assuming a dc conductivity is shown for comparison.

The wake is obtained by numerically inverse Fourier transforming the impedance. Since $\mathrm{Re}(Z)$ drops more quickly at high frequencies than $\mathrm{Im}(Z)$, it may be more convenient to use the cosine transform:

$$W(s) = \frac{2c}{\pi} \int_0^\infty \mathrm{Re}[Z(k)] \cos ks \, dk \ . \tag{9}$$

For $\Gamma \gtrsim 1$ and s not too large, the wake can be approximated by a simple, resonator wake [2]:

$$\begin{aligned} W(s) &\approx \frac{4}{a^2} e^{-s/4\Gamma s_0} \cos\left[(8/\Gamma)^{1/4} \, s/s_0\right] \\ &= \frac{4}{a^2} e^{-s/4c\tau} \cos\left[\sqrt{2k_p/a}\, s\right] \ , \end{aligned} \tag{10}$$

with the plasma frequency of the metal given by $k_p = \sqrt{4\pi\sigma/\tau}$. In Fig. 3 we plot the ac wake, its high Γ approximation (Eq. 10), and the dc wake, for comparison. We note that the ac wake rings much longer than the dc wake, and that Eq. 10 approximates the numerical ac result well over a relatively long distance. One can reduce the wake effect by using a metal with good dc conductivity and short relaxation time. Such a metal is aluminum, where $\sigma = 3.8 \times 10^{17}$/s and $c\tau = 2.4$ μm; $s_0 = 9.3$ μm and $\Gamma = 0.26$ for $a = 2.5$ mm. In Fig. 4 we plot the ac wakes of copper and aluminum, and the dc wake of copper. We note that the ac wake of aluminum is more rapidly damped than the ac wake of copper.

Given the wakefield, the relative energy change induced within a bunch is obtained from

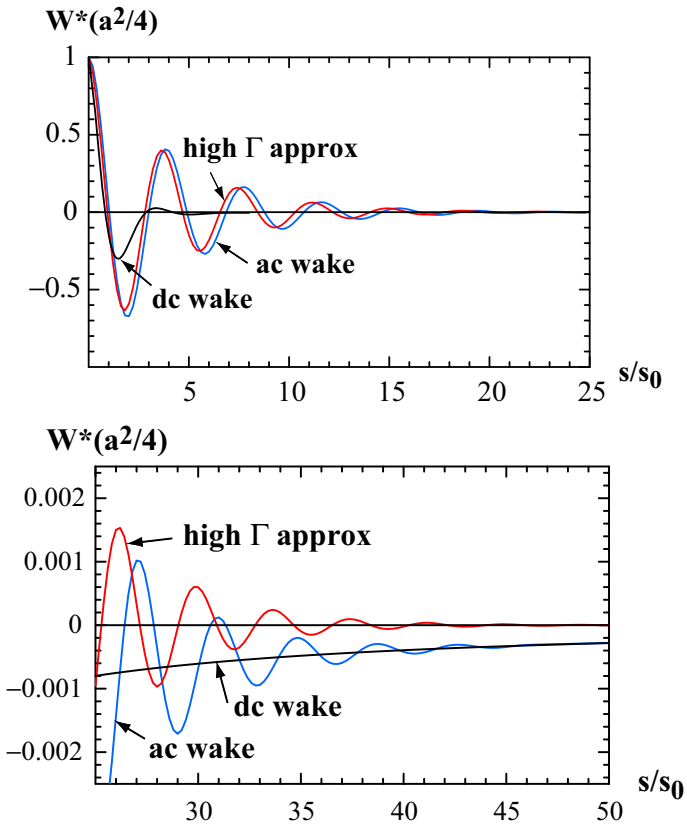

FIG. 3: The ac wake, its high Γ approximation, and the dc wake over the short range (top) and the longer range (bottom). Here $\Gamma = 1.0$.

the convolution

$$\frac{\Delta E}{E}(s) = -\frac{r_e N L}{\gamma} \int_0^\infty W(s')\lambda_z(s-s')\, ds' \ , \tag{11}$$

with $r_e = 2.8 \times 10^{-15}$m the classical electron radius, N the bunch population, L the length of the beam pipe, γ the Lorentz energy factor, and λ_z the longitudinal bunch distribution. (Note that a positive result indicates energy gain.) Using bunch properties given in Table I, and the bunch shape obtained from numerical simulations [4], we have calculated the voltage induced in the LCLS undulator beam pipe (see Fig. 5). Frame (a) gives the induced voltage assuming Cu-dc, Cu-ac, and Al-ac; frame (c) shows the longitudinal bunch shape, with head to the left. We see that particles within the horns have large energy variation; let us ignore these and focus on particles between the horns. Let us define as figure of merit δ_E, the total variation in energy change (maximum energy change minus minimum energy change) over that 30 μm length of beam that gives the minimum result. We see that with Cu-dc,

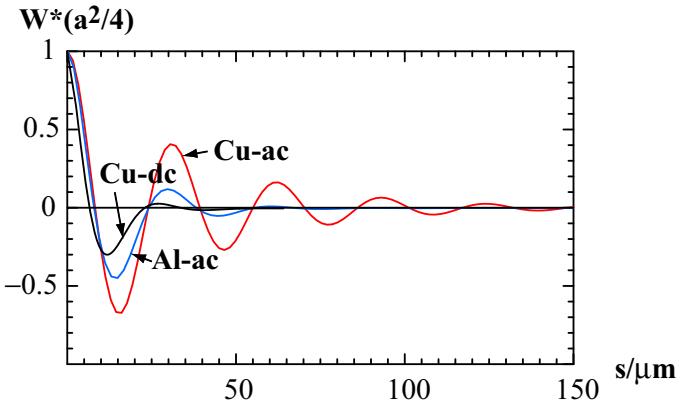

FIG. 4: The ac and dc wakes for copper, and the ac wake for aluminum, for the LCLS undulator beam pipe.

$\delta_E = 0.16\%$ (compare: the Pierce parameter is 5×10^{-4}), which appears to be acceptable according to FEL simulations [5]. The corresponding result for Cu-ac is large, 0.57%; for Al-ac it is 0.34%, which is better but still large. Finally, to get an idea of the dependence of the results on beam pipe radius we have repeated the calculations for double the radius, to $a = 5$ mm, and obtain (see Fig. 5b): for Cu-dc, $\delta_E = 0.07\%$, for Cu-ac, .017%, for Al-ac, 0.11%.

The LCLS bunch shape has leading and trailing horns, with a 3 kA flat region in between. To show the importance of the horns to the large ringing in the induced voltage, we repeat the induced energy calculation of Fig. 5, but now for a bunch with a uniform distribution, of peak current 3 kA and total length 60 μm (see Fig. 6; the vertical scale is the same as in Fig. 5). We note a significant reduction in induced energy variation. If we, for example, consider the middle 30 μm stretch of beam we now have energy deviation δ_E: for Cu-dc 0.05%, Cu-ac 0.23%, Al-ac 0.15%. If somehow the size of the leading horn can be reduced, we see that much can be gained.

Another effect that, in principle, can be important at high frequencies is the anomalous skin effect (ASE). It, in theory, applies whenever the mean free path $\ell = v_F \tau$ (v_F is the Fermi velocity) becomes large compared to the classical skin depth, given by

$$\delta_{sk} = \sqrt{\frac{c}{2\pi\sigma k}} \ . \tag{12}$$

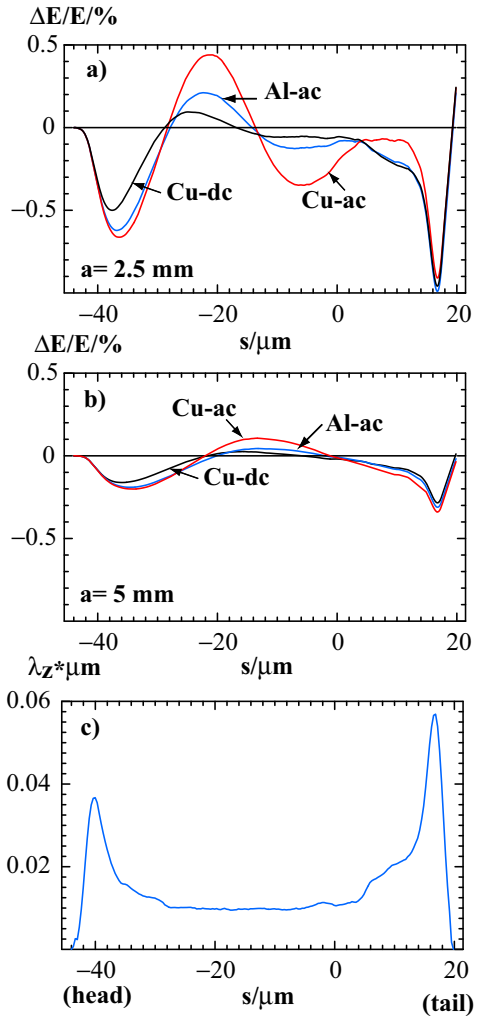

FIG. 5: Energy deviation induced in the LCLS bunch in the undulator with nominal beam pipe radius (a), and for $a = 5$ mm (b); the longitudinal bunch shape is given in (c).

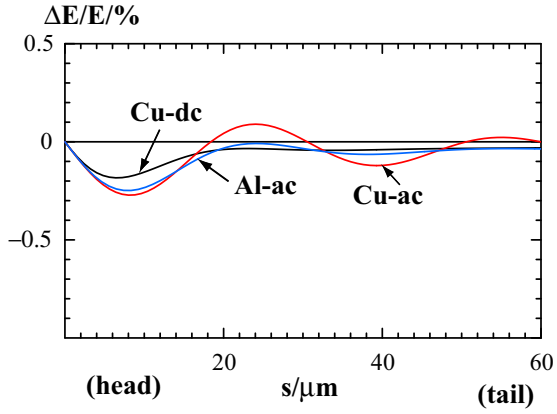

FIG. 6: Energy deviation induced by a uniform bunch distribution with peak current 3 kA and total length 60 μm.

At $k = (20\ \mu\text{m})^{-1}$ the skin depth and mean free path for copper are both 40 nm. The LCLS bunch, however, contains much higher frequencies due to the horns (for the leading horn $k \sim [2.5\ \mu\text{m}]^{-1}$), and one might expect ASE to be important. Nevertheless, ASE turns out to be important only at a low temperatures [6]. The reason is that (at room temperatures and) high frequencies, the condition for normal conductivity is that the path travelled by an electron during one period of field be small compared to the penetration depth, which is now approximately $c\sqrt{\tau/2\pi\sigma}$ (the ac conductivity $\tilde{\sigma} \approx \sigma/kc\tau$ is used in the equation for skin depth, Eq. 12); for any metal, as the frequency is increased, this will eventually be satisfied, and at frequencies lower than this point normal metals tend not to be very anomalous. Nevertheless, in Appendix A, following the theory of Reuter and Sondheimer [6], we obtain the wake, including the effect of ASE, for LCLS parameters. We show that, indeed, ASE is only a small perturbation on the ac wake results.

III. FLAT BEAM PIPE

Suppose, instead of a round beam pipe, we consider one with a flat or elliptical cross-section (wider than high) keeping the vertical aperture fixed. Could we in this manner reduce the wake effect in the LCLS undulator beam pipe? One would think that this might help: if we take the extreme case of two parallel plates, the long-range wake is the same as for the round case (if the distance between plates is $2a$), but the wake at the origin is reduced by the factor $\pi^2/16$ [7]. To investigate the benefit one might obtain from beam pipe cross-section change, we calculate here the impedance and wake, including ac conductivity, between two parallel plates (or at the center of a very flat, rectangular beam pipe) for LCLS parameters. Note that one consequence of having a non-round beam pipe is that the wakefield will depend on the beam's transverse position, though we confine ourselves here to beams on the symmetry plane.

Henke and Napoly obtained the dc impedance and short range resistive wall wake between two parallel plates [7]. Their result for impedance, in our notation, is [10]

$$Z(k) = \frac{1}{c}\int_{-\infty}^{\infty} dq \left[\frac{\lambda}{k}\cosh^2(qa) - \frac{ik}{q}\cosh(qa)\sinh(qa)\right]^{-1} , \tag{13}$$

where the parameter λ is the same as given before. We have simplified their equation by dropping small order terms. Note that the impedance looks similar to the round case, except that now we have an integral to perform numerically.

We have repeated the impedance and wake calculations for a flat chamber, for both dc and ac cases. The impedance for copper is given in Fig. 7 (compare with the round case, shown in Fig. 2; the scales are the same). Note that for the ac case the peaks in Re(Z) are lower and wider, than for the round case. The wakefields for Cu-ac, Cu-dc, and Al-ac are shown in Fig. 8 (compare with Fig. 4a). The wakes at the origin are smaller by a factor $\pi^2/16$, and the ac wakes damp more quickly (their Q factor is lower) and the oscillation period is longer than in the round pipe case. Note that the same behavior was found when comparing the wakes for flat and round geometry of a beam pipe with small, periodic corrugations [8]. In Appendix B we fit the short range ac wakes for both round and flat beam pipes to a simple damped oscillator, in order to quantify the short range wake behavior with Γ. We find, for example, in going from round to flat for the LCLS beam pipe with aluminum the effective frequency reduces from $ks_0 = 1.83$ to 1.31, and the Q factor from 1.66 to 1.33. Finally, in Fig. 9 we give the energy deviation induced in the LCLS bunch for the flat chamber (compare with Fig. 5a). For a 30 μm stretch of beam between the horns, the (minimum total) deviation in induced energy change for the ac results is $\sim 35\%$ better than for the round beam pipe: for Cu-ac $\delta_E = 0.39\%$, for Al-ac $\delta_E = 0.20\%$ (for Cu-dc it is 0.14%). The Al-ac deviation is about the same as for Cu-dc (round or flat), and acceptable. A summary of our results for the LCLS beam shape, for both round and flat beam pipes, is given in Table II.

IV. ACKNOWLEDGEMENTS

We thank P. Emma for discussions on the LCLS parameters, for supplying the LCLS bunch shape, and for carefully reading the manuscript, and B. Podobedov for information on the anomalous skin effect.

TABLE II: Total variation in energy change (maximum change minus minimum change) induced within the bunch within the 130 m LCLS undulator, δ_E, for different assumptions about the beam pipe shape and conductivity. Nominally the vertical aperture $2a = 5$ mm. In our calculations we consider the LCLS double horned bunch distribution; our results are for that 30 μm stretch of beam between the horns that minimizes the total variation. Note that Cu-dc results are not physically realizable.

Pipe Shape	Cu-dc	Cu-ac	Al-ac
Round	0.16%	0.57%	0.34%
Flat	0.14%	0.39%	0.20%
Round, $a = 5$ mm	0.07%	0.17%	0.11%

V. CONCLUSIONS

We have shown that, due to the ac resistive wall wakefield, the present LCLS undulator design, with its round copper beam pipe, will result in an unacceptably large energy variation induced within the bunch over the length of the undulator (0.6%). We have also shown that if, instead, we use a flat, aluminum chamber, the variation in induced energy can be reduced to within acceptable limits ($\lesssim 0.2\%$). And finally we have shown that the effect of the anomalous skin effect in the beam pipe wall is small, and can be ignored.

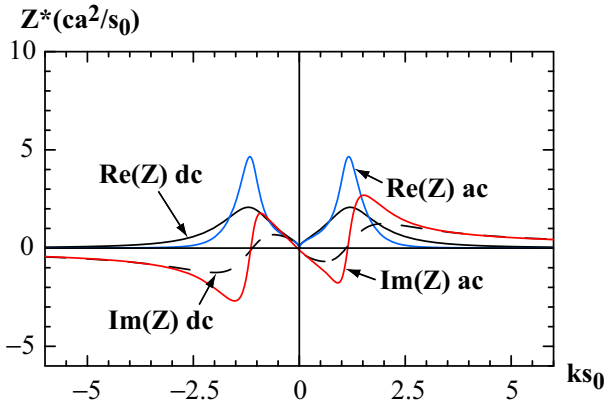

FIG. 7: For a flat chamber, the real and imaginary parts of impedance, including ac conductivity, for the LCLS undulator beam pipe. Here $\Gamma = 1.0$. The impedance assuming a dc conductivity is shown for comparison.

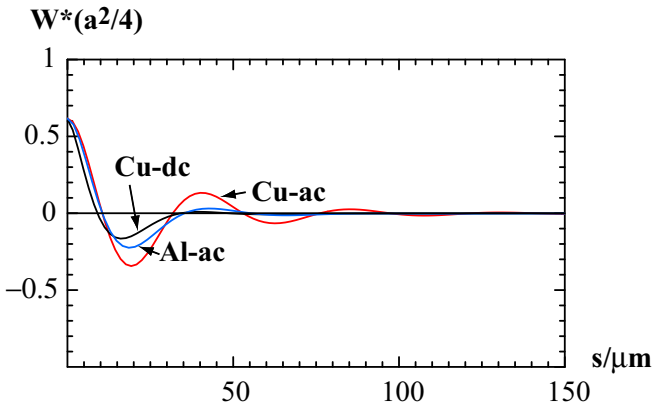

FIG. 8: For a flat chamber, the ac and dc wakes for copper, and the ac wake for aluminum, for the LCLS undulator beam pipe.

In our calculations, however, we have assumed ideal metal surfaces. We caution that the effect on dc conductivity or relaxation time of impurities, oxides, or roughness in the surface layer of the beam pipe wall may increase the induced energy variation by some amount. Therefore, it would seem prudent to have in the design space between the allowable energy variation and that expected from wakefield calculations. The ringing in the wake which causes the problem is driven strongly by the leading horn in the bunch distribution. One way to alleviate the problem (though it may not be feasable) would be to smooth out the leading horn in the charge distribution. If this is not possible, it may be advisable to rethink basic LCLS parameters, such as bunch charge, undulator gap, etc., in order to introduce overhead in the design.

VI. APPENDIX A: ANOMALOUS SKIN EFFECT

The general theory of the anomalous skin effect (ASE) was derived by Reuter and Sondheimer (R-S) [6]. R-S give their solution in terms of the surface impedance, defined as $Z_s = R_s + iX_s = 4\pi\mathcal{E}/c\mathcal{H}$, where $\mathcal{E}$ and $\mathcal{H}$ are the tangential electric and magnetic fields on the metal surface. First note that the classical (non-ASE) surface impedance is given by

$$R_{s,cl} = \sqrt{\frac{2\pi k}{c\sigma}}\sqrt{-kc\tau + \sqrt{1+k^2c^2\tau^2}} \tag{14}$$

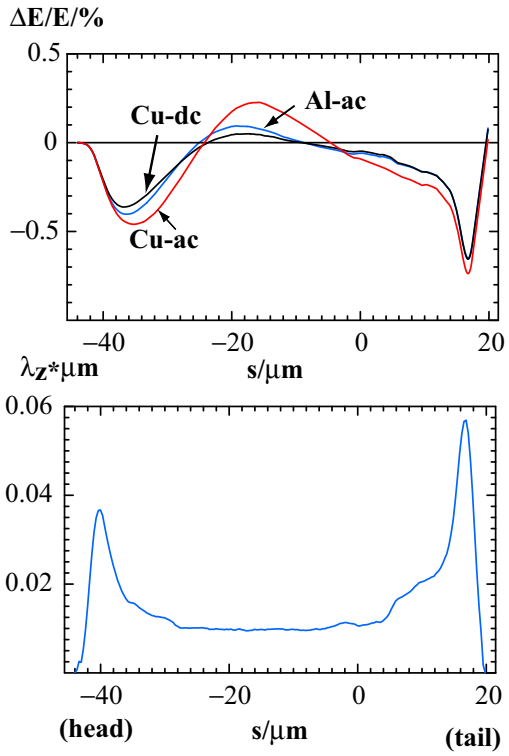

FIG. 9: For a flat chamber, the energy deviation induced in the LCLS bunch in the undulator (top); the bunch shape is given in the bottom frame.

$$X_{s,cl} = \sqrt{\frac{2\pi k}{c\sigma}}\sqrt{kc\tau + \sqrt{1+k^2c^2\tau^2}}\ . \tag{15}$$

The ASE surface impedance is

$$\frac{R_s}{R_{s,cl}} = \frac{4}{\pi}\sqrt{\frac{2\alpha}{3}}\frac{kc\tau\,\mathrm{Re}(I) - \mathrm{Im}(I)}{(1+k^2c^2\tau^2)\sqrt{-kc\tau + \sqrt{1+k^2c^2\tau^2}}} \tag{16}$$

$$\frac{X_s}{X_{s,cl}} = \frac{4}{\pi}\sqrt{\frac{2\alpha}{3}}\frac{\mathrm{Re}(I) + kc\tau\,\mathrm{Im}(I)}{(1+k^2c^2\tau^2)\sqrt{kc\tau + \sqrt{1+k^2c^2\tau^2}}} \tag{17}$$

with

$$I = \int_0^\infty \frac{dt}{t^2 + \frac{2i\alpha}{(1+ikc\tau)^3}\frac{[(1+t^2)\tan^{-1}t - t]}{t^3}}\ . \tag{18}$$

R-S's ASE strength parameter is defined as $\alpha = \frac{3}{2}(\ell/\delta_{sk})^2$. We can define a dimensionless anomalous strength parameter, one that is independent of frequency, $\Lambda \equiv \alpha/kc\tau$. Finally, note that the equations here are for specular (mirror) reflection off the metal surface. Formulas have been derived also for diffuse reflection, though, according to R-S, the quantitive difference is small.

The impedance for a round beam pipe is obtained by inserting

$$\lambda = \frac{4\pi|k|/c}{R_s\,\mathrm{sgn}(k) - iX_s} \tag{19}$$

into Eq. 2. The wakefield is then obtained, as before, by numerically taking the inverse Fourier transform of Z. In Fig. 10 we plot the ratios $R_s/R_{s,cl}$ (solid) and $X_s/X_{s,cl}$ (dashes) *vs.* frequency for two values of the anomalous skin effect parameter Λ. For Λ on the order of unity we see that the effect is small. For copper at room temperature $\Lambda = 3.4$ and the peak of $R_s/R_{s,cl} = 1.2$. In Figs. 11–12 we plot the impedance and wakefield when the anomalous skin effect is included in calculations, and compare with the non-ASE results. We note that the anomalous skin effect does not change the results significantly.

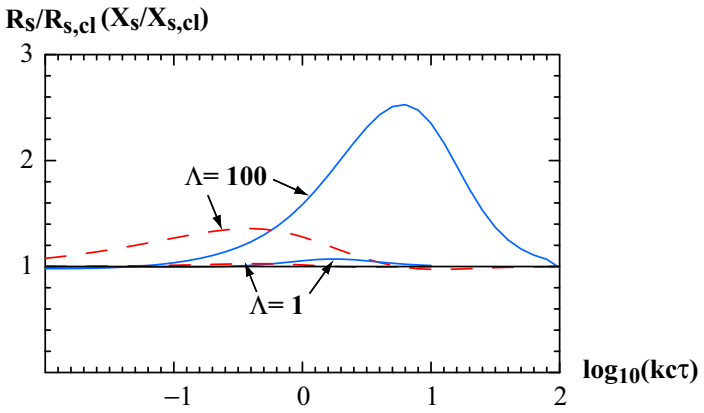

FIG. 10: The ratios $R_s/R_{s,cl}$ (solid) and $X_s/X_{s,cl}$ (dashes) *vs.* frequency for two values of the anomalous skin effect parameter Λ.

Finally, note that ASE behaves quite differently at low temperatures (sometimes called the extreme anomalous regime [EASE]) than at room temperature. Although the formalism given here is still correct, the equations simplify greatly. For the EASE regime, where the anomalous skin effect *is* important, the impedance and wake of a beam pipe have been obtained by B. Podobedov[9].

VII. APPENDIX B: PARAMETER STUDY OF AC WAKES

We here explore the Γ dependence of the short range ac wake, for both round and flat beam pipes, by fitting to a simple function. Note that a similar study was done for the

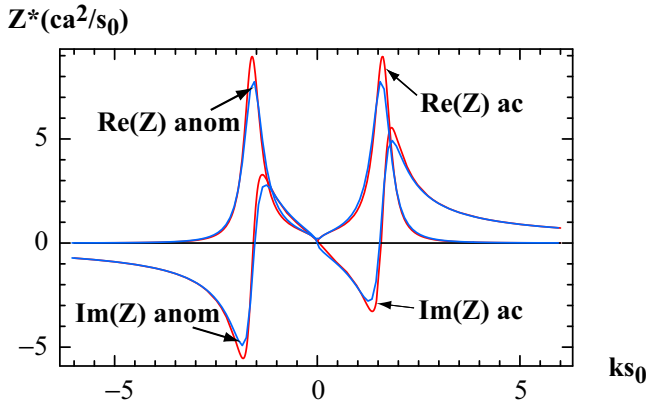

FIG. 11: Impedance of round, copper LCLS beam pipe when including the anomalous skin effect (blue), or ac conductivity only (red). Note $s_0 = 8.1$ μm, $\Gamma = 1.0$, and $\Lambda = 3.4$.

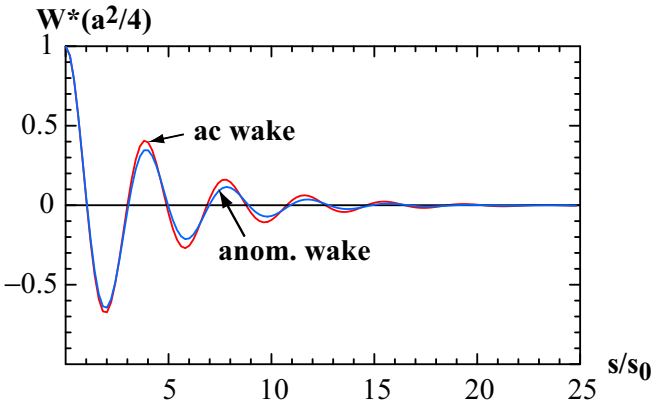

FIG. 12: Wake of round, copper LCLS beam pipe when including the anomalous skin effect (blue), or ac conductivity only (red). Note $s_0 = 8.1$ μm, $\Gamma = 1.0$, and $\Lambda = 3.4$.

round case in Ref. [2].

The short range ac wakes have a dependence on s that is similar to a damped oscillator. To quantify the Γ dependence of the short range wakes we, therefore, fit to a simple damped oscillator model: $W = 4a^{-2}e^{-k_r s/2Q_r}\cos(k_r s)$, with k_r and Q_r the fitting parameters, for the round case; for the flat case, the model wake is a factor $\pi^2/16$ smaller. The fitting is actually performed in frequency space, and we fit (up to $ks_0 = 6$) Re(Z), that has been numerically obtained as described in the text, to the real part of the Fourier transform of the damped resonator model. As goodness of fit indicator we take r_{err}, the square root of the estimated variance, divided by the peak of Re(Z).

In Fig. 13 we show again the wakes of Figs. 4 and 8 (the solid curves) and compare with the fits to the resonator model (the dashes). We see that the fits are reasonably good over the short range; for larger Γ values (consider the Cu-ac curves), the fits become better.

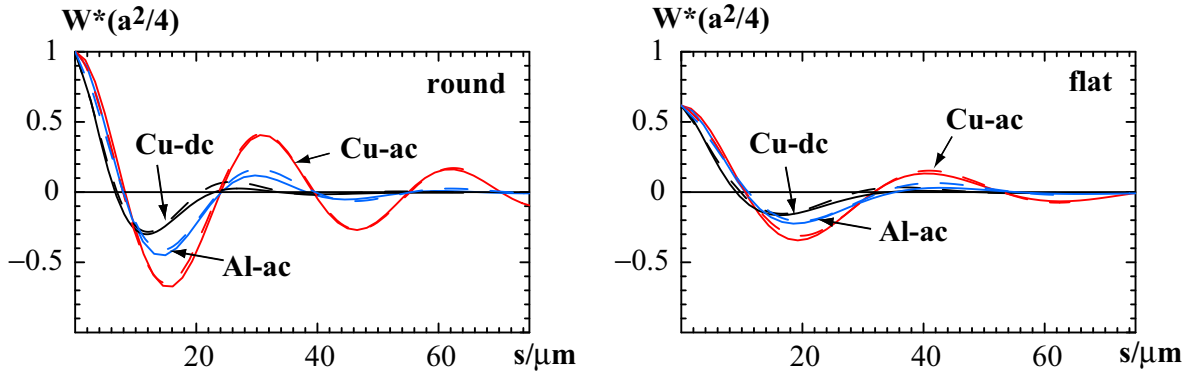

FIG. 13: The ac and dc wakes for copper, and the ac wake for aluminum for the LCLS undulator beam pipe, for the round (left) and flat (right) case. Dashes show how well the simple resonator fit works. For Cu $s_0 = 8.1$ μm, Al $s_0 = 9.3$ μm; for Cu-dc $\Gamma = 0$, Cu-ac $\Gamma = 1.0$, Al-ac $\Gamma = 0.26$.

In Fig. 14 we summarize our fitting results. Shown are the fitted k_r and Q_r, and the goodness of fit parameter r_{err} for both round and flat beam pipes. Also shown, by the dashed curves, are the large Γ approximations for the round case, $k_r s_0 = (8/\Gamma)^{1/4}$ and $Q_r = \Gamma(8/\Gamma)^{1/4}$ (see Eq. 10), which we see agree well for $\Gamma \gtrsim 1$. We see that, for both types of beam pipes, as Γ increases the fitted k_r drops, Q_r increases, and the fit becomes better (r_{err} drops). Comparing the flat to the round case, we note that the frequency k_r is smaller (by $\sim 1/\sqrt{2}$) and Q_r is also smaller. For the flat case, by fitting we obtain the approximation $Q_r \approx 2.4 \log(\Gamma + 1.5)$. For example, for the LCLS undulator copper beam pipe ($\Gamma = 1$), from going from round to flat, the wake frequency drops from $k_r s_0 = 1.6$ to 1.2, and the damping from $Q_r = 3.5$ to 2.2.

REFERENCES

[1] N. Ashcroft and N. Mermin, *Solid State Physics* (Harcourt Brace College Publishers, Orlando, FL, 1976).

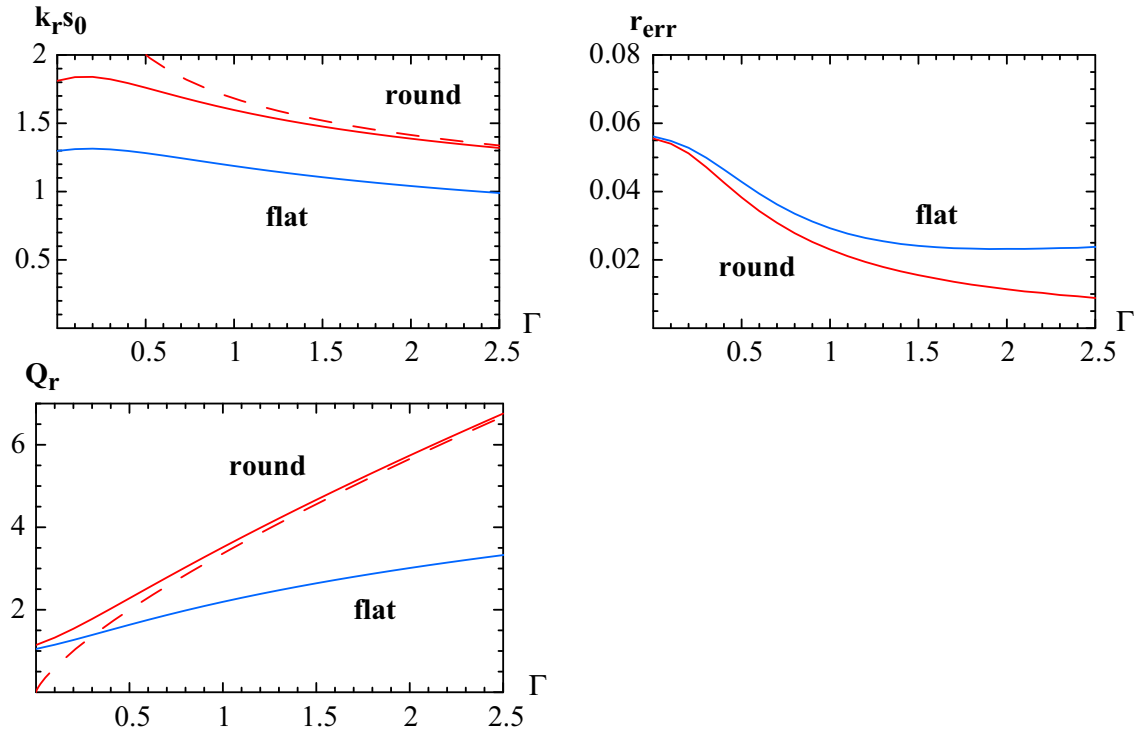

FIG. 14: Fitting parameters k_r (top left) and Q_r (bottom left), and goodness of fit indicator r_{err} (top right) as functions of Γ, for round (red) and flat (blue) beam pipes. The dashed curves give the high Γ approximations for the round case: $k_r s_0 = (8/\Gamma)^{1/4}$ and $Q_r = \Gamma(8/\Gamma)^{1/4}$.

[2] K.L.F. Bane and M. Sands, in *Proc. of the Micro Bunches Workshop, Upton, NY* (1995).

[3] A. W. Chao, *Physics of collective beam instabilities in high energy accelerators* (John Wiley & Sons, New York, NY, 1993).

[4] P. Emma, private communication.

[5] S. Reiche, talk at mini-workshop "Start to end simulations of x-ray FEL's," held at Zeuthen, Germany, August 2003; http://www.desy.de/s2e.

[6] G. Reuter and E. Sondheimer, Proc. of the Royal Society of London **A195**, 336 (1949).

[7] H. Henke and O. Napoli, in *Proceedings of the 2nd European Particle Accelerator Conference, Nice, France, 1990* (Editions Frontières, Nice, France, 1990).

[8] K. Bane and G. Stupakov, Physical Review Special Topics–Accelerators and Beams

6(024401) (2003).

[9] B. Podobedov, talk given at SLAC, January 2004.

[10] We believe that there is a factor $1/4\pi$ typo in their Eq. 16.